Journal of Zhejiang University-SCIENCE A (Applied Physics & Engineering)
ISSN 1673-565X (Print); ISSN 1862-1775 (Online)
www.zju.edu.cn/jzus; www.springerlink.com
E-mail: jzus@zju.edu.cn

Lower extremity injuries in vehicle-pedestrian collisions using a legform impactor model

A. ABVABI†1, A. NASR†2, A. NOORPOOR1, M. S. KIASAT3
([1]Department of Automotive Engineering, Iran University of Science and Technology, Tehran, Iran)
([2]School of Railway Engineering, Iran University of Science and Technology, Tehran, Iran)
([3]Faculty of Marine Technology, Amirkabir University of Technology, Tehran, Iran)
†E-mail: a_abvabi@auto.iust.ac.ir; a_nasr@iust.ac.ir
Received Mar. 25, 2009; Revision accepted Sept. 24, 2009; Crosschecked Oct. 12, 2009

Abstract: Though the bumper of a vehicle plays a major role in protecting the vehicle body against damage in low speed impacts, many bumpers, particularly in large vehicles, are too stiff for pedestrian protection. In designing a bumper for an automobile, pedestrian protection is as important as bumper energy absorption in low speed collisions. To prevent lower extremity injuries in car-pedestrian collisions, it is important to determine the loadings that car front structures impart on the lower extremities and the mechanisms by which injury is caused by these loadings. The present work was focused on gaining more insight into the injury mechanisms leading to both ligament damage and bone fracture during bumper-pedestrian collisions. The European Enhanced Vehicle-safety Committee (EEVC) legform impactor model was introduced and validated against EEVC/WG17 criteria. The collision mechanism between a bumper and this legform impactor was investigated numerically using LS-DYNA software. To identify the effect of the bumper beam material on leg injuries, four analyses were performed on bumpers that had the same assembly but were made from different materials.

Key words: Finite element model (FEM), Legform impactor, Pedestrian safety, Lower extremity injury, Composite bumper
doi:10.1631/jzus.A0900169 **Document code:** A **CLC number:** O34

1 Introduction

Pedestrians comprise more than 33% of the 1.2 million people killed and 10 million injured annually in road crashes (Crandall *et al.*, 2002). About 12%–35% of fatal or severe injuries from road traffic accidents are suffered by pedestrians, while pedestrians are involved in only 4%–8% of all accidents (Svoboda and Cizek, 2003).

The National Highway Traffic Safety Administration (NHTSA) (Lee and Abdel-Aty, 2004) announced that the numbers of pedestrians killed and injured in the United States in 2003 were 4700 and 70000 respectively (Lee and Abdel-Aty, 2005). Most serious or fatal injuries occur at low vehicle speeds of between 25 and 50 km/h. Lower extremity and pelvis injuries are the most frequent types of injury (Svoboda *et al.*, 2003).

Vehicle structures have been developed in recent years to protect the occupants in a vehicle collision. This has led to the development of high strength vehicle bodies which deform to absorb energy during an impact, protecting the occupants from high forces. Euro NCAP (2004) carried out different tests to examine the strength of vehicle bodies and the safety of a vehicle for its occupants. As a result of these efforts, the number and severity of automobile occupant injuries are now on the decline. Research into pedestrian protection has been carried out since the early 1960s (Yong and Young, 2002). However, the protection of pedestrians has received less attention.

Although the number of fatal injuries to pedestrians has decreased, the pedestrian crash risk may not have been reduced because more people use their own cars and the use of public transportation systems has increased. A pedestrian's injury risk in a collision with a vehicle is dependent on several parameters, such as vehicle speed, vehicle body characteristics and the direction of vehicle movement. In pedestrian-vehicle crashes, the windshield and bumper are two critical parts that may cause serious injuries to the head and lower limbs.

To predict pedestrian injuries resulting from impacts with cars, full scale dummy and pedestrian subsystem tests are used. The European Enhanced Vehicle-safety Committee (EEVC) proposed a subsystem test procedure to assess the protection that vehicles provide to pedestrians during a collision. In EEVC/WG17, the pedestrian protection test consists of three impact tests: the headform impactor to bonnet top test, the lower legform impactor to bumper test and the upper legform impactor to bonnet leading edge test.

Current investigations focus on pedestrian leg injuries, because the leg is the most vulnerable body part in nonfatal pedestrian accidents (about 38% of all injuries) (Matsui, 2005).

The EEVC procedure uses a legform impactor developed by the Transport Research Laboratory (TRL). A legform impactor is imposed on the bumper at a velocity of 40 km/h in a direction parallel to the longitudinal axis of the vehicle, and the lower leg acceleration, knee shearing displacement and knee bending angle are measured (EEVC/WG17). The lower leg acceleration is used to evaluate the tibia crack risk, while the knee shear displacement and bending angle are used to evaluate the ligament injury risks.

To reduce the severity of pedestrian lower limb injury, two approaches were identified: designing more friendly bumpers for pedestrians by changing the material and geometry of bumper structure, and using exterior airbags in bumper assembly (Schuster, 2006).

Several experimental and numerical studies were performed in different countries to assess the aggressiveness of a bumper in a car-pedestrian accident. A computer model for pedestrian subsystem impact tests was introduced by the Road Vehicles Research Institute (TNO) and Japan Automobile Research Institute (JARI) in Japan (Konosu *et al*., 2000). The Japan Automobile Manufacturers Association (JAMA) and JARI have begun the development of a more complex legform that is able to simulate the flexibility of the human long bone and that has a mechanical knee joint that is a closer replication of a human knee. This is the only alternative legform impactor, as compared with the EEVC/WG17 legform impactor proposed by Lawrence *et al*. (2004). There are some environmental conditions that affect test results from EEVC legform impactors. For instance, with an increase in the relative humidity in the legform impactor dynamic certification test, the maximum acceleration will be increased (Matsui and Takabayashi, 2004). It is now accepted that the bumper structure of a vehicle plays a major role not only in protecting the vehicle from body damage in low speed impacts but also in reducing pedestrian injuries. Hence, efforts were focused on designing an optimum bumper. Davoodi *et al*. (2008) presented a conceptual design of a polymer composite automotive bumper energy absorber for pedestrian safety.

To achieve pedestrian safety requirements, different parts of a vehicle body can be changed and their effects on safety analyzed. The legform impactor introduced in this paper consists of fewer components to reduce the analysis time. The legform consists of an artificial femur, tibia, skin and flesh. For the knee joint only a beam element is used. In a similar model, Dutton and Solihull (2003) used solid elements with added masses to simulate the knee joint. Using this legform impactor model, the accuracy of results obtained in EEVC dynamic and static certification tests are acceptable. In pedestrian-bumper collisions, the stiffness of the vehicle front structure is important in investigating the effect of bumper beam material on pedestrian injuries. Thus, the introduced legform impactor was used in collision with different bumper beams. The main goal of the present study was to investigate the effect of bumper beam material on pedestrian lower limb injuries by introducing a new legform dynamic model.

2 Structure of the legform impactor and its modeling

Considering previous studies and other legform impactors that have been used for pedestrian safety analyses, there are some points that should be considered: e.g., similar legform impactor models are often commercial and no precise relevant engineering data are available for use by other researchers. In this study, the geometrical and mechanical properties of different parts and the method for modeling a legform impactor are described in detail for the first time in the literature. The main idea in our proposed legform impactor model is to introduce a simple model using a few components to achieve acceptable results in a relatively short time. In some legform impactor models, the results achieved in the required standard static and dynamic tests are not applicable to the whole range of applications. This is considered in the present work. Changing the stiffness of bumper assembly and providing some new insight into the crush depth are two important means for reducing pedestrian injuries. Clearly, in the design of a new vehicle, the designer should have a general understanding of the effect of bumper beam material on lower extremity injuries and the maximum acceptable stiffness of bumper assembly. This could be achieved using the new legform impactor presented in this study.

Pedestrian protection is a worldwide concern, especially in European countries. The European Enhanced Vehicle Safety Committee (EEVC/WG10 and WG17) proposed a component subsystem test for cars to assess pedestrian protection (Fig. 1).

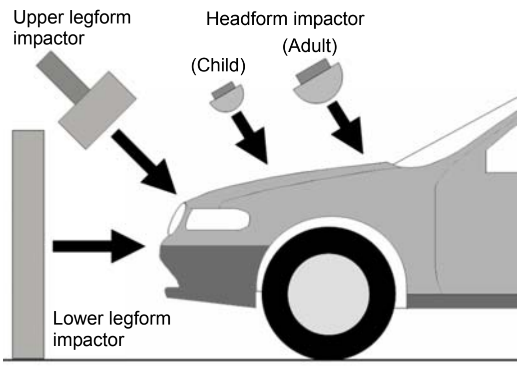

Fig. 1 EEVC pedestrian subsystem impact test features (EEVC/WG17)

To determine the aggressiveness of a bumper using a legform impactor, impact is imposed at 40 km/h horizontally in line with the automobile. The lower leg acceleration, knee shearing displacement and knee bending angle are measured (Fig. 2).

The femur and tibia are represented by two cylinders, each of 70 mm outer diameter. The geometrical properties of the femur and tibia, such as mass, moments of inertia and center of gravity, are specified in the EEVC/WG17 report. The femur and tibia are covered by artificial flesh and skin. Confor foam (CF-45), and neoprene are used for modeling the flesh and skin, respectively.

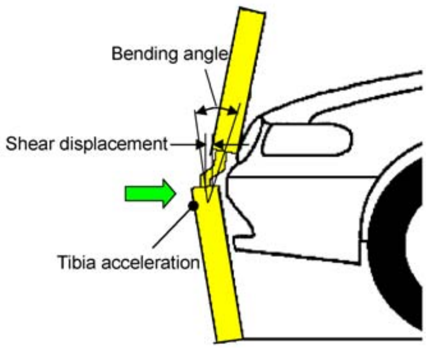

Fig. 2 Standard measurement parameters (EEVC/WG17)

To validate the legform impactor, the EEVC/WG17 static and dynamic test procedures were used.

The bones of the femur and tibia of the legform impactor were modeled using shell elements. After modeling the geometry of the legform impactor for achieving the required mass, two lump masses in special locations were used to tune the masses in the center of gravity of the femur and tibia.

As specified in EEVC/WG17, the total masses of the femur and tibia shall be (8.6±0.1) kg and (4.8±0.1) kg, respectively. By considering the mass densities ρ=96.11 kg/m^3 and 1100 kg/m^3 of CF-45 foam and neoprene skin, respectively, the exact masses of bone of the femur and tibia were calculated.

A 6-kg and a 2-kg lump mass were placed in the femur and tibia, respectively, so as to locate the center of gravity of these parts, as specified in EEVC/WG17. The locations of these lump masses (z_1 and z_2) are shown in Fig. 3.

By calculating the moment of inertia in this model and by using the lump moment of inertia at the center of gravity of the femur and tibia, the moment of inertia specified in the EEVC/WG17 report was achieved. The added moments of inertia at the center of gravity of the femur and tibia were 0.08611 and 0.0556 kg·m^2, respectively.

The geometrical properties of different parts of the legform impactor are shown in Table 1.

The particular problem here is the characteristics of the knee joint between the femur and tibia and those of the foam and skin. The knee joint was modeled using a 6-DOF discrete beam. The shearing of the knee was represented by a linear force-versus-displacement curve and the bending response of the

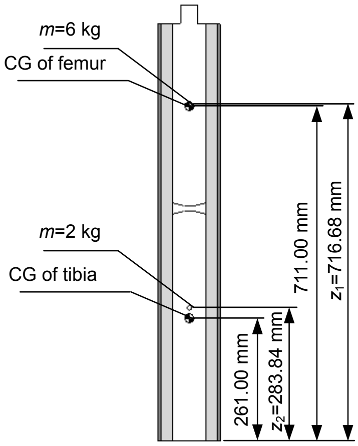

Fig. 3 Locations of added lump masses in the femur and tibia

z_1 and z_2 are distances from added masses to the lower point of tibia and CG refers to center of gravity

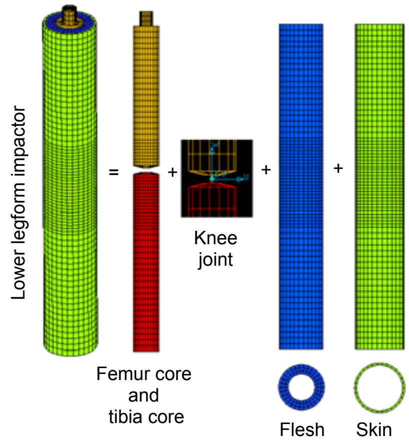

Fig. 4 Finite element model of the legform impactor

Table 1 Geometrical properties of the femur and tibia

Property	Femur	Tibia
Added lump mass (kg)	6	2
Distance of added lump mass from lower point of tibia (mm)	716.68	283.84
Added lump moment of inertia in respective CG (kg·m^2)	0.08611	0.0556
Total mass (kg)	8.6	4.8
Total moment of inertia about the horizontal axis (kg·m^2)	0.127	0.120

knee was represented by a nonlinear moment-versus-rotational-displacement curve. Different degrees of freedom of the knee joint were tuned so that the static and dynamic characteristics were achieved.

Solid elements with low density foam material (LS-DYNA material type 57) were selected for modeling CF-45 foam. The mechanical properties of foam material were specified by Cappetti *et al.* (2006) and Yao *et al.* (2008). The skin was modeled using solid elements with viscoelastic material. The mechanical properties of the skin were obtained from Konosu (2006).

Some degree of vibration was observed in dynamic certification analysis. This was prevented using a translational damper (c is the damping coefficient, 500 N·s/m) in the knee joint of the legform impactor. For achieving reliable results, mesh density in the impact area was refined and smaller mesh elements were used. After the modeling of flesh and skin, the finite element model (FEM) of the legform impactor was achieved (Fig. 4).

3 Validation of the legform impactor

To validate the legform impactor, the EEVC/WG17 static and dynamic standard test procedures were used. The results are discussed below. The resulting angle of knee deflection in the static bending validation test was recorded (Fig. 5). During this analysis, the force-versus-angle results were within the standard upper and lower limits and the energy taken to generate 15.0° of bending was 98.79 J, which is also within the EEVC/WG17 permitted criterion (100±7) J. The resulting knee shearing displacement in the static shearing certification test is shown in Fig. 6. The results were within the upper and lower standard limits during the analysis.

The legform impactor dynamic certification test is shown in Fig. 7. Here, cables were modeled using beam elements and cable discrete beam material.

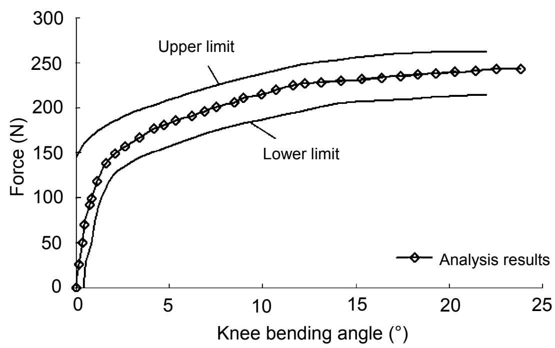

Fig. 5 Force versus angle in the static bending certification test

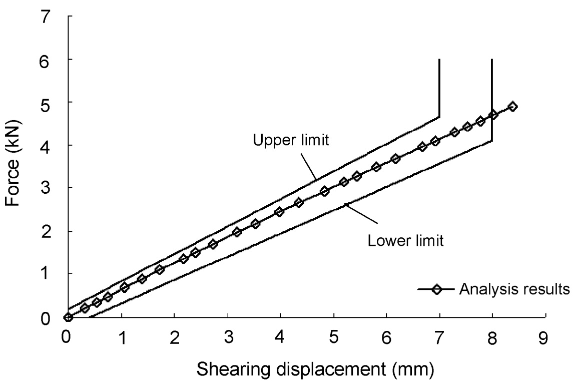

Fig. 6 Force versus displacement in the static shearing certification test

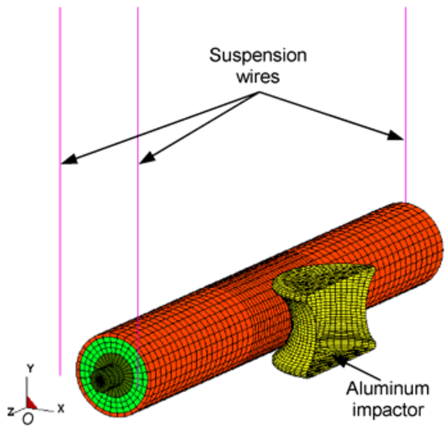

Fig. 7 Dynamic certification test

The deformation of the legform impactor in the dynamic certification test is shown in Fig. 8. The time when the maximum levels of the three parameters occurred was close to that recorded by Dutton and Solihull (2003) for a similar legform model. The results of the dynamic test (Table 2) were all within the EEVC/WG17 acceptable criteria. The accuracy of the results obtained was in some cases considerably better than that of the results obtained using other models (Fig. 9).

Table 2 Results achieved from the dynamic certification test

	Upper tibia acceleration (×g)	Maximum bending angle (°)	Maximum shearing displacement (mm)
Analysis result	211.23	7.93	5.41
EEVC criterion	120–250	6.2–8.2	3.5–6.0

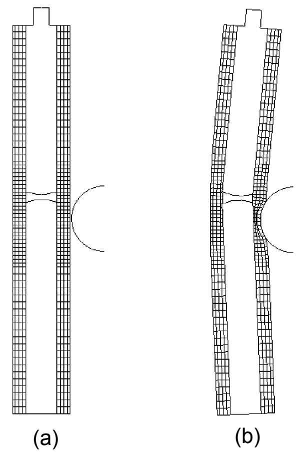

Fig. 8 Deformation of the legform impactor in the dynamic certification test. (a) Before deformation; (b) After deformation

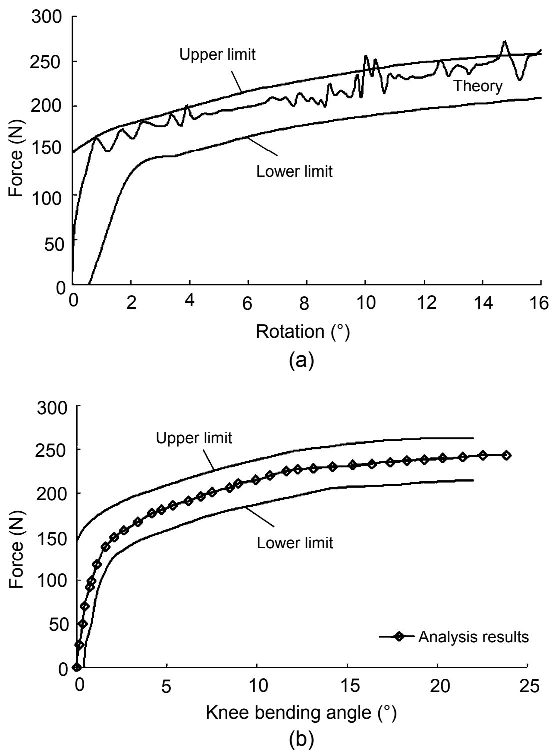

Fig. 9 Comparison of knee bending static test results between (a) another similar model (Dutton and Solihull, 2003) and (b) our model

Thus, all mechanical and physical properties and calculated results from the static and dynamic tests were in agreement with those specified in the EEVC/WG17 and hence the legform impactor model introduced in the present study can be used for pedestrian safety tests.

4 Results and discussion

4.1 Effect of bumper beam material on lower extremity injuries

The legform dynamic model can be used in pedestrian safety tests. To do this, a bumper assembly of a sedan vehicle was also modeled. In terms of the EEVC/WG17 description, the lower and upper bumper heights were 405 and 533 mm, respectively. The bumper structure consisted of a bumper beam, shock absorbers and a bumper skin (Fig. 10). The shock absorbers were made of polypropylene copolymer and the bumper skin of Hifax 238 (a non-filled polypropylene copolymer). Four different materials, i.e., steel, aluminum, glass mat thermoplastic (GMT) and sheet molding compound (SMC), were selected for the bumper beam. The geometry of the bumper assembly and test conditions in all four analyses were the same. Table 3 shows the material properties of these parts. By performing four crash analyses, the effect of bumper beam material on pedestrian safety was investigated. The legform-bumper impact was imposed at 40 km/h velocity parallel to the longitudinal axis of the vehicle, and initial conditions of analyses were as specified in EEVC/WG17. Fig. 11 shows the legform-bumper collision. In the FEM of these analyses, the rear nodes of the bumper structure attaching the bumper to other parts of the body were clamped. An impact was imposed on the center of the bumper and three important parameters of the legform were recorded. According to the EEVC/WG17 pedestrian test, the maximum permitted knee bending angle criterion, knee shearing displacement and upper tibia acceleration are 15°, 6 mm and 150g (g=9.81 m/s^2), respectively. Fig. 12 shows the deformation of the bumper assembly and the legform during GMT bumper-legform collision.

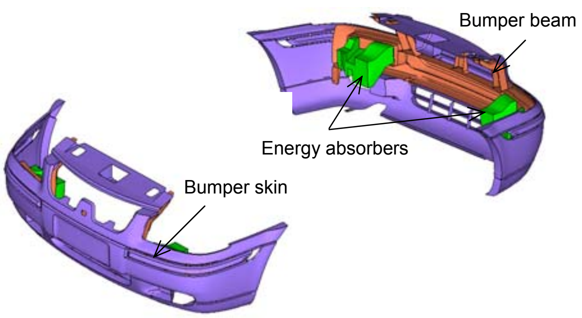

Fig. 10 Different parts of the bumper assembly

Table 3 Mechanical properties of different parts of the bumper assembly

Part	Material	ρ (kg/m^3)	E (GPa)	σ_y (MPa)	υ
Bumper skin	Hifax 238	900	1.145	24.5	0.37
Energy absorbers	Polypropylene copolymer	900	1.34	27	0.392
Bumper beam	Steel	7850	210	700	0.3
	Aluminum	2710	70	480	0.33
	GMT	1240	5.6	90	0.36
	SMC	1900	15	170	0.25

ρ, E, σ_y and υ are the density, Young's modulus, yielding stress and Poisson's ratio, respectively

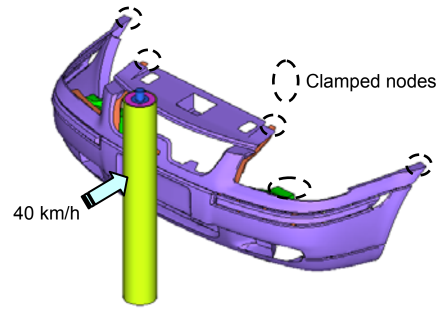

Fig. 11 Collision between the legform and the bumper

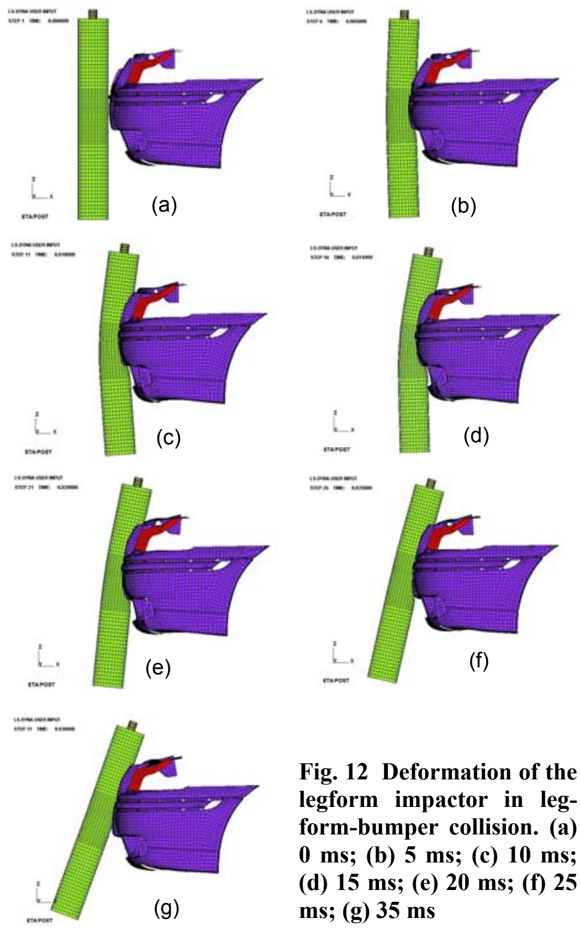

Fig. 12 Deformation of the legform impactor in legform-bumper collision. (a) 0 ms; (b) 5 ms; (c) 10 ms; (d) 15 ms; (e) 20 ms; (f) 25 ms; (g) 35 ms

The knee bending angle in four analyses is shown in Fig. 13. The maximum knee bending angle in the GMT bumper was within the EEVC acceptable criterion and by changing the material and increasing the strength of the bumper beam, the maximum knee bending angle increased. The maximum bending angles from steel, aluminum and SMC bumpers were not within the EEVC limit, a result critical to pedestrian safety. As the strength of the bumper beam was increased, the bumper assembly resisted free movement and the bending angle in the legform increased. In all analyses, the maximum knee bending angle occurred at 10−14 ms after collision. Then, by decreasing the kinetic energy of the legform, the bumper assembly pushed the legform in a reverse direction and the knee bending angle decreased.

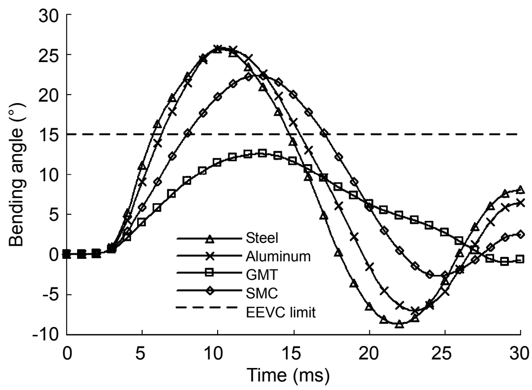

Fig. 13 Knee bending angle resulting from collisions with different bumper beams

The knee shearing displacement and upper tibia acceleration for these different materials are shown in Fig. 14 and Fig. 15, respectively. The knee shearing displacement was within the EEVC acceptable criterion in all analyses and this parameter is not critical for this bumper. By using materials of higher strength, the initial relative motion of the femur and tibia is reversed. This is because with high strength bumper beam materials, the bumper beam offers more resistance against the free movement of the femur, and therefore the movement of the tibia in the direction of the collision is greater than that of the femur. But in composite bumper beams of lower strength, the movement of the femur in the direction of the collision is greater than that of the tibia. This is because of the geometry of bumper assembly and the distribution of bumper stiffness, as discussed above. The knee shearing displacement is related to the bumper geometry and the distribution of bumper stiffness near the knee joint.

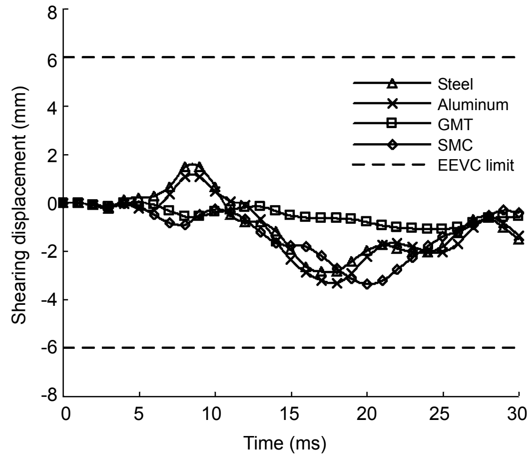

Fig. 14 Knee shearing displacement resulting from collisions with different bumper beams

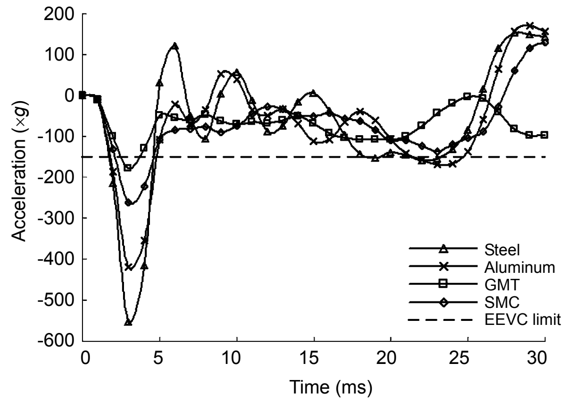

Fig. 15 Upper tibia acceleration resulting from collisions with different bumper beams

The upper tibia acceleration increased as the strength of the bumper beam material was increased (Fig. 15). In all analyses, the maximum upper tibia acceleration occurred at about 3 ms after collision, following an increase in acceleration. The maximum upper tibia acceleration is important for pedestrian safety. When the legform impactor was impacted by high strength bumper beams, there was higher stiffness in the bumper beam and very little deformation in the bumper assembly, so upper tibia acceleration increased.

In this study, the upper tibia acceleration was not within the EEVC criterion in four analyses. The energy distribution and required spring constant for the bumper beam could be investigated as follows.

The total impact energy at 40 km/h is

$$E_c = \frac{1}{2}mv^2 = \frac{1}{2}\times 13.4\times 11.11^2 = 827.16, \quad (1)$$

and the force required for acceleration with up to 150*g* in the legform is

$$F_{max} = ma_{max} = 13.4\times(150\times 9.81) = 19718.1, \quad (2)$$

where E_c, m, v, F_{max} and a_{max} are kinetic energy, mass, velocity, maximum force on the legform model and maximum acceleration of the legform model, respectively, and units of E_c and F_{max} are J and N, respectively.

The kinetic energy should be calculated from the integration of the load-displacement diagram:

$$E_c = \int F\mathrm{d}s, \quad 827.16 = 19718.1\times S_{max}, \quad S_{max} = 41.94. \quad (3)$$

Therefore, the required spring constant for the bumper beam is

$$K = \frac{F_{max}}{S_{max}} = \frac{19718.1}{41.94} = 470.15, \quad (4)$$

where S_{max} is the maximum displacement of the bumper beam, mm, and K is the stiffness of the bumper beam, N/mm.

Hence, the maximum bumper beam spring constant to prevent excess acceleration is 470.15 N/mm.

Fig. 16 shows the internal energy in the bumper beam in four case analyses. When the legform impactor was impacted by the bumper assembly, the kinetic energy of the legform decreased and this energy was distributed through the bumper assembly. By movement of the bumper beam, its internal energy increased, reached a peak and then, when the kinetic energy of the legform impactor decreased and the legform moved in a reverse direction, the total internal energy decreased. As impact energy is absorbed by the bumper beam, lower extremity injuries will be reduced. Clearly, a good bumper assembly for pedestrian safety should absorb more energy during collision. The GMT bumper was the best and the steel bumper the worst in this regard. However, plastic energy in the GMT bumper beam is high and hence the relevant damage is severe. Furthermore, to identify the bumper beam damage, von Mises stress in bumper beams was investigated. The maximum von Mises stress in the GMT bumper is shown in Fig. 17. von Mises stress shows that yield occurred in the GMT bumper beam. In other analyses yield stress occurred in SMC bumpers but there is no evidence of any yield in steel or aluminum beams.

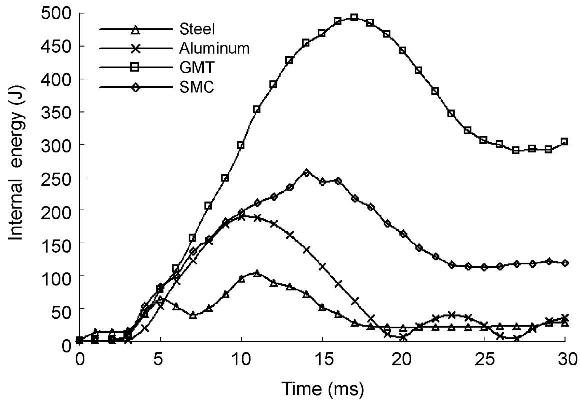

Fig. 16 Internal energy in the bumper beam vs. material

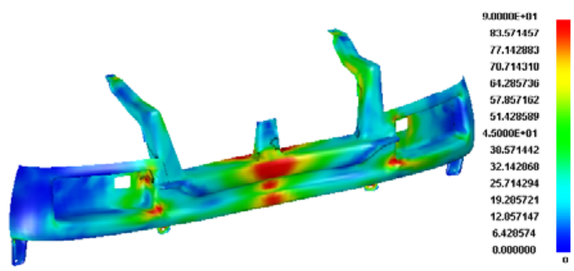

Fig. 17 Maximum von Mises stress in the GMT bumper beam

The bumper low speed test is very important and those materials that perform well in pedestrian safety are usually not so good in low speed tests. One of the aims of vehicle body design is the optimization of bumper assembly.

For pedestrian safety, GMT material is the best choice. In legform collision with the GMT bumper, the knee bending angle and knee shearing displacement were 12.57° and 1.107 mm, respectively, both less than the standard limits of 15° and 6 mm, respectively.

5 Conclusion

In nonfatal passenger vehicle pedestrian accidents, the lower extremities are the body parts most commonly injured. Car manufacturers usually use a legform impactor test for designing better and more friendly car structures. In legform impactor models, many components are necessary to achieve accurate models. The advantage of the legform impactor model used in the present study is its simplicity and its use of optimized components. Moreover, the accuracy of the results obtained was in some case considerably better than that obtained using other models. In designing a new vehicle, time is very important. By this simple model, the total analysis time is reduced and different analyses can be performed so that the optimum design can be achieved in a short time.

Different bumper beam materials were used in this study to gain more insight into the effect of material on injury mechanisms. As investigated, for pedestrian safety the bumper beam should absorb more energy. By using a bumper beam of lower strength, upper tibia acceleration, the knee bending angle and the knee shearing displacement in the legform impactor are reduced. When the legform impactor is impacted by high strength bumper beams (with high stiffness in the bumper beam) deformation is very small. This causes the upper tibia acceleration to increase. As shown in this study, to prevent a high acceleration in the legform, the bumper beam stiffness should be less than 470.15 N/mm. The GMT material is the best choice for pedestrian safety. However, by using this material yield stress will occur in the bumper beam. Low speed impact tests should be investigated to obtain a more comprehensive assessment.

References

Cappetti, N., Donnarumma, A., Naddeo, A., Russo, L., 2006. Design of experiment about foam CF45 for pedestrian safety in car design. *Journal of Materials Processing Technology*, **175**(1-3):77-82. [doi:10.1016/j.jmatprotec.2005.04.045]

Crandall, J.R., Bhalla, K.S., Madeley, N.J., 2002. Designing road vehicles for pedestrian protection. *BMJ*, **324**(7346):1145-1148. [doi:10.1136/bmj.324.7346.1145]

Davoodi, M.M., Sapuan, S.M., Yunus, R., 2008. Conceptual design of a polymer composite automotive bumper energy absorber. *Materials and Design*, **29**(7):1447-1452. [doi:10.1016/j.matdes.2007.07.011]

Dutton, T., Solihull, A., 2003. Finite Element Models for European Testing: Side Impact Barrier to WG13-Pedestrian Impactors to WG17. 4th European LS-DYNA Users Conference, Ulm, Germany, p.29-48.

European Enhanced Vehicle-safety Committee (EEVC), 1998. Improved Test Methods to Evaluate Pedestrian Protection Afforded by Passenger Cars. EEVC Working Group 17 Report.

Euro NCAP (European New Car Assessment Program), 2004. Version 4.1.

Konosu, A., 2006. Information on the Flexible Pedestrian Legform Impactor GT Alpha (Flex-GTα). 3rd Flex-TEG MT, Bast, Bergisch.

Konosu, A., Ishikawa, H., Kant, R., 2000. Development of computer simulation models for pedestrian subsystem impact tests. *Society of Automotive Engineers of Japan*, **21**(1):109-115.

Lawrence, G., Hardy, B., Carroll, J., Donaldson, W., Visvikis, C., Peel, D., 2004. A Study on the Feasibility of Measure Relating to the Protection of Pedestrians and Other Vulnerable Road Users. Transport Research Laboratory.

Lee, C., Abdel-Aty, M., 2005. Comprehensive analysis of vehicle—pedestrian crashes at intersections in Florida. *Accident Analysis and Prevention*, **37**(4):775-786. [doi:10.1016/j.aap.2005.03.019]

Matsui, Y., 2005. Effects of vehicle bumper height and impact velocity on type of lower extremity injury in vehicle pedestrian accidents. *Accident Analysis and Prevention*, **37**(4):633-640. [doi:10.1016/j.aap.2005.03.005]

Matsui, Y., Takabayashi, M., 2004. Factor causing scatter in dynamic certification test results for compliance with EEVC WG17 legform impactor standard. *International Journal of Crashworthiness*, **9**(1):5-13.

Schuster, P.J., 2006. Current trends in bumper design for pedestrian impact. *Society of Automotive Engineering*, **1**:464.

Svoboda, J., Cizek, V., 2003. Pedestrian–vehicle collision: vehicle design analysis. *Society of Automotive Engineering*, **1**:0896.

Svoboda, J., Solc, Z., Cizek, V., 2003. Analysis of collision between pedestrian and small car. *International Journal of Crashworthiness*, **8**(3):269-276. [doi:10.1533/ijcr.2003.0239]

Yao, J.F., Yang, J.K., Otte, D., 2008. Investigation of head injuries by reconstructions of real-world vehicle-versus-adult-pedestrian accidents. *Safety Science*, **46**(7):1103-1114. [doi:10.1016/j.ssci.2007.06.021]

Yong, H., Young, W., 2002. Optimization of bumper structure for pedestrian lower leg impact. *Society of Automotive Engineering*, **1**:23.